Membrane protein degradation is intrinsic to vacuole fusion

Joël Denis Richard

A Thesis
in
The Department
of
Biology

Presented in partial fulfillment of the requirements
for the degree of Master of Science (Biology) at
Concordia University
Montréal, Quebec, Canada

September 2013

CONCORDIA UNIVERSITY
School of Graduate Studies

This is to certify that the thesis prepared

By: Joël Denis Richard

Entitled: Membrane protein degradation is intrinsic to vacuole fusion

and submitted in partial fulfillment of the requirements for the degree of

Master of Science (Biology)

complies with the regulations of the University and meets the accepted standards with respect to originality and quality.

Signed by the final Examining Committee:

_____ Chair
Dr. Robert Weladji

_____ Examiner
Dr. Alisa Piekny

_____ Examiner
Dr. Vladimir Titorenko

_____ External Examiner
Dr. Luc Varin

_____ Supervisor
Dr. Christopher Brett

Approved by:

_____
Chair of Department or Graduate Program Director

_____ 2013 _____

Dean of Faculty of Arts and Science

ABSTRACT

Membrane protein degradation is intrinsic to vacuole fusion

Joël Denis Richard

In eukaryotic cells, integral membrane protein (IMP) turnover is an important contributor to cell physiology. Whereas the only known mechanism for IMP degradation is the multivesicular body (MVB) pathway, there are examples of IMPs that eschew this pathway and travel directly to the vacuole surface, suggesting that a second mechanism acts at the vacuole. Previously, it was shown that homotypic vacuole fusion yields an intralumenal membrane fragment within the fusion product, providing the cell with a unique opportunity to internalize (and thus, degrade) a portion of vacuolar membrane and its protein cargoes. Based on this result, we hypothesized that vacuole IMPs are sorted for internalization during the sub-reactions that lead to vacuole fusion. Using epifluorescence microscopy, I confirmed that Fth1-GFP and Ybt1-GFP localize exclusively to the vacuole membrane, and are sorted into, or out of, respectively, the membrane domain that is internalized upon homotypic vacuole fusion. Additionally, I demonstrated that Mup1, a surface methionine transporter, colonizes the vacuole limiting membrane upon disruption of the MVB pathway, and also becomes internalized during homotypic vacuole fusion. This study provides the first evidence of a novel selective IMP degradation mechanism, which works independently or complementarily to the MVB pathway. Further studies are required to confirm whether vacuole IMPs are sorted based on their ubiquitylation status (as in the MVB pathway), or whether the vacuole fusion protein machinery has a role within this process.

ACKNOWLEDGEMENTS

First, I would like to formally acknowledge and thank my labmates Mahmoud Karim and Dipti Patel for the preparation of proteins and reagents necessary for my experiments; as well as Gabriel Lapointe for help with fluorescence microscopy and morphometric analysis.

Second, on a more personal note, I would like to thank my brother Alby, my mother Jackie, and my partner Taylor for their patience and support, without which I surely could not have completed this degree.

Finally, I would like to thank my supervisor Chris for providing, both in word and deed, superlative mentorship.

TABLE OF CONTENTS

LIST OF FIGURES

LIST OF TABLES

INTRODUCTION

Integral membrane proteins (IMPs) – such as surface receptors or ion transporters – are vital for cell signaling and substrate transport across membranes, and constitute cargoes within various intracellular trafficking pathways. Generally speaking, in the yeast *Saccharomyces cerevisiae*, IMPs are delivered by the secretory pathway, and degraded by the endocytic pathway, whose terminal organelle is the vacuole (Li and Kane, 2009). The low-pH vacuole lumen contains many hydrolytic enzymes and activator proteins that degrade membranous inputs (Sarry et al., 2007), whose constituent molecules are then exported back to the cytosol for further use in cell metabolism. Regulation of IMP levels is thus a dynamic and important contributor to cell physiology, and understanding how IMPs are degraded is crucial to achieve a comprehensive understanding of the same.

The MVB pathway

The only known selective IMP degradation pathway is the multivesicular body (MVB) pathway (Henne et al., 2011), which culminates with the deposition of cargo-laden endosomal vesicles into the vacuole. Following the pioneering work of the Stevens group (Raymond et al., 1992) – whose classical genetic screens uncovered the vacuole protein sorting (VPS) genes – the Emr group quickly elucidated the protein machinery that drives the MVB pathway, starting with the late-acting Vps4 (Babst et al., 1997), and followed by the endosomal sorting complex required for transport (ESCRT) complexes, ESCRT-I (Katzmann et al., 2001), ESCRT-II and -III (Babst et al., 2002a; Babst et al., 2002b), and finally the early-acting ESCRT-0 complex (Katzmann et al., 2003). A brief overview of the MVB pathway follows.

First, the ESCRT-0 complex (Vps27 and Hse3) localizes to the endosome via its affinity for phosphatidylinositol 3-phosphate (PI3P), where it simultaneously recognizes ubiquitylated IMP cargoes and recruits the ESCRT-I complex (Vps23, Vps28, Vps37, Mvb12) through its interaction with Vps23. ESCRT-I, through its Vps23 subunit, also interacts with ubiquitylated cargoes. The ESCRT-II complex (Vps36, Vps22, Vps25) is recruited by Vps28, and propagates the sorting process through its Vps36 subunit, which also has an affinity for ubiquitylated cargoes, as well as PI3P. The ESCRT-III complex (Vps20, Snf7, Vps24, Vps2), whose Snf7 subunit forms filamentous oligomers, then sequesters ubiquitylated cargoes into membrane patches that start to bud into the endosome lumen. Eventually, the Vps4/Vta1 complex is recruited by Vps24 and Vps2, which cap the Snf7 oligomers. Vps4 is a AAA-type ATPase, and serves to catalyze the step whereby the invaginated membrane is severed, creating an intralumenal vesicle (ILV) within the endosome. The creation of ILVs is a hallmark of maturation from the early to the late endosome, which is otherwise called the MVB. The pathway functionally culminates when the MVB fuses with the vacuole, depositing many cargo-loaded ILVs into the caustic vacuole lumen, and fulfilling the promise of IMP degradation first imparted by their previous post-translational modification with a ubiquitin (Ub) moiety (Urbanowski and Piper, 2001; Shields and Piper, 2011).

Another IMP degradation pathway must exist

Three observations point to the existence of another membrane degradation pathway. First, cells can grow and reproduce when key MVB pathway components have been deleted (Raymond et al., 1992). Second, previous reports indicate cargo degradation that bypasses the MVB pathway, without naming an alternative mechanism (Bowers et al., 2006; Theos et al., 2006). Third, certain IMPs, such as those who follow the Golgi-to-

vacuole pathway (Cowles et al., 1997; Burd et al., 1998), are never trafficked to the endosome, and thus lack a fully elucidated mechanism of turnover.

In order to demonstrate the existence of a new degradation pathway, candidate cargoes must be investigated with respect to three criteria, as seen within the MVB pathway. Cargoes must (1) be *sorted* into a restricted domain on the limiting membrane of an endocytic compartment that (2) becomes *internalized* into the lumen of an endocytic compartment, so that (3) the cargo is eventually exposed to the acid hydrolases within the vacuole, and thus *degraded*.

Homotypic vacuole fusion produces an internal membrane fragment

A model of organelle maturation can be used to describe the movement of IMP cargoes through the endocytic pathway: Once surface cargoes are internalized into vesicles, these vesicles fuse to form early endosomes, which then mature into late endosomes (MVBs), which then fuse with the vacuole. That is to say, membrane fusion events drive the anterograde trafficking of IMP cargoes in this pathway, which ends with the vacuole. The premier system to study organelle fusion is the yeast vacuole, and for nearly two decades the Wickner group (and its academic offspring) have used this system to build and curate a detailed model for this process.

Vacuole fusion (Wickner, 2010) proceeds in four distinct steps. "Priming" prepares vacuoles for their initial attachment – referred to as "tethering" – which continues as "docking", a process that draws vacuoles together into the apposed topology that precedes "fusion", which is characterized by a complete mixing of lumenal contents. A brief overview of each step follows.

Priming is defined as the disassembly of *cis*-SNARE (soluble *N*-ethylmaleimide-sensitive factor attachment receptor) complexes by Sec17 (a SNARE specific chaperone) and Sec18 (a AAA-type ATPase) on the vacuole membrane, which frees the individual SNAREs (Vam3, Vti1, Vam7, Nyv1) from their fully complexed state and allows them to partially bind their cognate SNAREs in *trans* on apposing vacuoles (Mayer et al., 1996).

Tethering is defined as the instance that two vacuole membranes make first contact, and is generally regarded as the only reversible step. Tethering requires the vacuole specific Rab-GTPase Ypt7 and its effector, the homotypic fusion and protein sorting (HOPS) holocomplex (Ungermann et al., 1998b; Seals et al., 2000; Hickey et al., 2009; Lo et al., 2012), which is comprised of the class-C core complex (Vps11, Vps16, Vps18, Vps33) decorated with two accessory proteins (Vps39 and Vps41). Tethering involves the interaction between the active, GTP-bound version of Ypt7 – which is membrane-anchored due to its C-terminal prenylation (Calero et al., 2003) – and the HOPS holocomplex, whose EM/tomography-based, low-resolution structure indicates that its accessory proteins – which interact with active Ypt7 (Wurmser et al., 2000; Brett et al., 2008) – are at the far end of an elongated complex (~30nm) that bulges at its ends, and is flexible in the middle (Bröcker et al., 2012). Although tethering is thought only to involve Ypt7-Ypt7 (Lo et al., 2012) or Ypt7-HOPS (Bröcker et al., 2010) interactions, it is worth noting that HOPS, through its Vps16, Vps18, and Vps33 subunits, has an affinity for the N-termini of three vacuolar SNAREs: Vti1 and Vam3, which are membrane spanning, and Vam7, which is soluble, but also able to interact with PI3P at its opposite C-terminus (Boeddinghaus et al., 2002; Kramer and Ungermann, 2011; Xu and Wickner, 2012).

Docking is the stage whereby tethering proceeds, and involves the iterative recruitment of additional tethering factors (i.e. HOPS, Ypt7), as well as nascent *trans*-interacting SNARE bundles, to the expanding point of membrane contact, referred to as the vertex. Recruitment is driven by the synergic interplay of Ypt7 and HOPS with the Mon1/Ccz1 complex (Wang et al., 2003a; Nordmann et al., 2010), a guanosine exchange factor (GEF) that promotes the transition from inactive to active Ypt7. As a result of this interplay, the vertex is thought to start as a point and expand radially as a ring while its structure is stabilized by the stringent interaction between HOPS and correctly aligned, nascent *trans*-SNARE complexes (Wang et al., 2003b; Starai et al., 2008). In addition, regulatory lipids of fusion (Mayer et al., 2000; Kato and Wickner, 2001; Jun et al., 2004), as well as PI3P (which interacts with Vam7) are also known to interdependently concentrate at the site of membrane contact (Fratti et al., 2004), which suggests that the vertex is a highly ordered microdomain (**Figure 1A**). Other regulators of docking include Gyp3 and Gyp7, both of which are GTPase activating proteins (GAPs) that promote the inactivation of Ypt7 (Eitzen et al., 2000; Lachmann et al., 2012), and Gdi1, a GDP dissociation inhibitor that binds to and extracts inactive Ypt7p from the vacuole membrane (Ignatev et al., 2008). These proteins serve to mitigate the radial expansion of the vertex prior to fusion by coordinating the recruitment of additional tethering factors.

Fusion involves the mixing of apposed phospholipid bilayers along the vertex (Wang et al., 2002), driven by the complete 'zippering' of nascent *trans*-SNARE complexes – whose full association surrenders enough energy to overcome the hydrophobic barrier inherent to this process (Gao et al., 2012). As a result, *trans*-SNARE complexes are converted to *cis*-SNARE complexes on the surface of the now-fused

vacuole. Finally, Sec17 displaces HOPS from these *cis*-SNARE complexes in anticipation of Sec18 (Ungermann et al., 1998a), which starts the fusion cycle anew.

Because fusion occurs along the vertex of membrane contact, it deposits a significant portion of vacuolar membrane into the lumen of the resulting fused vacuole product (Wang et al., 2002). This necessitates the definition of topological domains in addition to the vertex microdomain (see **Figure 1A**): Membranes not in contact during docking are termed "outside" membranes, whereas apposed membranes within the vertex ring are referred to as "boundary" membranes, and are said to constitute the "contact zone" that is internalized upon vacuole fusion.

The discovery that vacuole fusion deposits vacuolar membrane into the lumen elicits an obvious comparison to the functional conclusion of the MVB pathway, where membrane is both *internalized* and *degraded*. The implication is clear; the cell is bestowed a unique opportunity to *selectively* (perhaps via the fusion protein machinery) dispose of vacuolar membrane and its protein constituents. Thus, the vacuole fusion pathway is a viable candidate for a novel mechanism of regulated IMP degradation.

Can the fusion machinery sort IMPs for degradation?

Although active sorting of IMPs into the contact zone has not previously been demonstrated, two observations suggest that protein sorting may occur during vacuole fusion. First, given its highly organized nature (Wang et al., 2003b; Fratti et al., 2004), the vertex microdomain likely acts as a steric barrier that could regulate IMP movement into (or out of) the contact zone. Second, some IMPs, like Vph1 (a constituent of the V-ATPase proton pump) have already been observed within the contact zone (Wang et al., 2002), demonstrating the possibility of protein inclusion within this domain. I therefore

propose that the vacuole fusion machinery has an important function apart from its role in fusion: That of sorting IMP cargoes for degradation by shunting them (or not) into the internalized membrane fragment that results from vacuole fusion (**Figure 1B**).

To test this hypothesis, I used fluorescence microscopy to identify GFP-labeled IMPs that may be sorted and degraded by this process. I discovered two biosynthetic cargoes (or resident vacuole IMPs), Fth1 and Ybt1, that are sorted by this process. Additionally, I showed that once the MVB pathway is abrogated, the MVB cargo Mup1 colonizes the vacuole membrane and gets internalized upon vacuole fusion. This last result indicates that both pathways may share a common sorting mechanism (i.e. ubiquitylation), and most likely work cooperatively in order to maximize the efficiency of cargo degradation.

Figure 1. Model depicting how cargoes may be sorted during docking

(**a**) Within the vertex microdomain, HOPS (Vps11, Vps16, Vps18, Vps33, Vps39, Vps41) orchestrates a series interactions with its up and down stream effectors (the SNARE proteins Nyv1, Vam3, Vam7, and Vti1, the Rab-GTPase Ypt7, and its guanosine exchange factor, the Mon1-Ccz1 complex), which initiate tethering and drive docking. (**b**) Tethering occurs when HOPS and Ypt7 make their first contact in *trans* between apposed vacuoles. Docking refers to the progression of tethering, whereby the vertex microdomain radially expands with the addition of more tethering factors. Because the docking machinery is densely concentrated along this vertex, it is ideally placed to act as a sieve that allows certain IMP cargoes into the contact zone that is internalized upon fusion (for clarity, cargoes are shown on the surface of the bottom vacuole only).

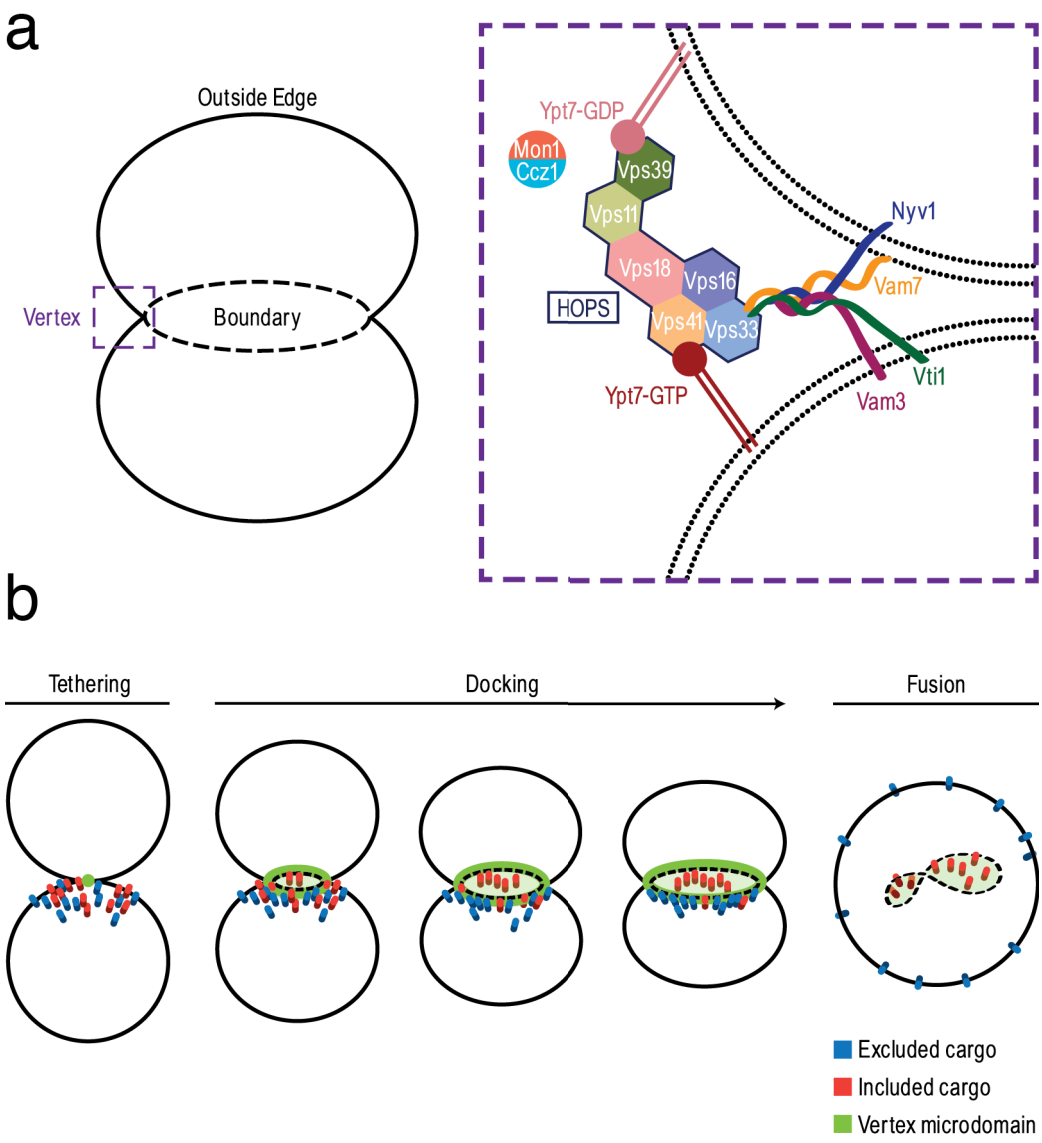
a
Outside Edge
Vertex
Boundary
Ypt7-GDP
Mon1
Ccz1
Vps39
Vps11
Vps18
Vps16
HOPS
Vps41
Vps33
Ypt7-GTP
Nyv1
Vam7
Vti1
Vam3
b
Tethering
Docking
Fusion
Excluded cargo
Included cargo
Vertex microdomain

MATERIALS & METHODS

Yeast experimental procedures

The *Saccharomyces cerevisiae* strains used in this study are listed in **Table 1**. All yeast cultures were grown at 30°C in rich media (YPD, 1% yeast extract, 2% peptone, 2% dextrose), or synthetic complete minimal media (SC, 0.67% yeast nitrogen base, 2% dextrose, amino acids and vitamins as needed), unless otherwise indicated. Liquid cultures were grown with rotary agitation at 200 rpm for aeration, and 1% agar was added to the medium for colony growth on plates. Gene deletions were effectuated by homologous recombination with the His3-MX6, TRP1, or KanMX6 selectable markers using PCR-derived cassettes containing 80 base pair overhangs with homology to the flanking regions of a targeted coding sequence, as previously described (Longtine et al., 1998). PCR primers are listed in **Table 2**. Deletion cassettes were transformed into parent yeast strains using standard lithium acetate methods based on Schiestl and Gietz (1989), and selected for on either histidine- or tryptophan-lacking SC agar plates, or YPD agar plates supplemented with 280mg/L G418 (Sigma-Aldrich), respectively. Gene deletions were confirmed by PCR amplification of the deleted loci using isolated genomic DNA obtained by lysing cells via glass bead disruption (3 min., using ~100 mg of acid-washed 500 µm beads) followed by standard phenol/chloroform extraction, based on Chomczynski and Sacchi (1987). PCR reactions were carried out as per manufacturer specifications (New England Biolabs) using 200 µM dNTPs, 0.2 µM forward and reverse primers, and milliQ dH_2O. Phusion® DNA polymerase (1 unit/50 µl reaction) + HF Phusion Buffer (1.5 mM $MgCl_2$, other constituents undisclosed) was used for cassette construction, whereas Taq DNA polymerase (1.5 units/50 µl reaction) + Standard Taq Buffer (10 mM Tris-HCl, 50 mM KCl, 1.5 mM $MgCl_2$, pH 8.3) was used for integrant

screening. All PCRs were analyzed by ethidium bromide staining and 1% agarose gel electrophoresis.

Vacuole isolation and reconstituted fusion

Vacuoles were isolated and fused *in vitro* as previously described (Haas et al., 1994). Briefly, cells were spheroplasted with Zymolyase® (Nacalai USA, Inc.), and centrifuged for 90 min. at 125,000 g on a 15/8/4/0% Ficoll® (GE Healthcare) gradient dissolved in PS buffer (20 mM Pipes-KOH pH 6.8, 200 mM Sorbitol). Isolated vacuoles were harvested from the 4/0% interface, and quantified using the Bradford assay (Thermo Scientific), based on Bradford (1976). For each 30 µl *in vitro* fusion reaction, 6 µg of vacuoles per yeast strain were incubated at 27°C for all time points. Reaction constituents were mixed with PS buffer, and include KCl (0.125 M), $MgCl_2$ (5 mM), CoA (coenzyme A, 10 µM), and ATP (adenosine triphosphate salt; 1 mM).

Epifluorescence microscopy

To visualize vacuoles within intact yeast cells, cells were stained with the vital dye FM4-64 using a pulse-chase protocol first developed by Vida and Emr (1995). Briefly, 0.4 ml of a seed culture grown overnight in SC medium at 30°C was added to 4ml of YPD medium containing 0.5 µl of a 5 mM FM4-64 stock in DMSO (50 µM final), then grown for 1 hour at 30°C to facilitate cellular dye uptake via endocytosis. Afterwards, cells were pelleted (4500 rpm, 1 min), washed with 1 ml SC medium, resuspended in 3 ml SC medium, and grown for another 1-2 hours at 30°C before imaging, allowing the dye to accumulate in vacuole compartments. For isolated vacuole imaging, 0.5 µl of FM4-64 stock was added to freshly isolated vacuoles, which were then incubated at 27°C for 10 min., and placed on ice prior to imaging, as in Wang et al. (2002). Preparing samples for

imaging entailed sandwiching 6 µl of live cell or isolated vacuole suspension between two glass coverslips. All micrographs are the product of at least two independent viewing sessions, and were acquired at room temperature using 100× (for live cell) or 150× (for isolated vacuoles) magnification, with a Nikon Eclipse Ti-E fully-automated inverted epifluorescence microscope outfitted with a Photometrics Evolve 512 EMCCD camera and NIS Elements AR4.0.1 software (full specifications are available at http://cmac.concordia.ca). Image analysis was performed using ImageJ v1.48a (National Institutes of Health; NIH) and Photoshop CS5 (Adobe Systems), where original micrographs were subjected to fluorescence intensity normalization prior to the application of colour inversion, and an unsharpen mask filter (80%, 4.0 pixel radius, threshold = 3).

Morphometric analysis

To examine cargo sorting within docked vacuole clusters, morphometric data was acquired as previously described (Wang et al., 2002) using ImageJ v1.48a (NIH), processed using Excel 2011 (Microsoft), and presented using Kaleidagraph v4.1.3 (Synergy). Briefly, micrographs were split into their FM4-64 and GFP channels and each resulting image was background subtracted using the mean fluorescence + 1 standard deviation from the same 'empty' (i.e. without any vacuoles) area proximal to a vacuole cluster. Images were converted to 32-bit (floating point) format to avoid any loss of data in the subsequent steps. Pixel intensity values were then converted to logarithmic values for each image, and the FM4-64 image was subtracted from the GFP image according to the pixel math LogF – LogG = LogR, where F represents FM4-64 fluorescence, G represents GFP fluorescence, and R is the ratio of the two. Measurements were

redirected to the resulting ratiometric image, and the FM4-64 image (which typically had the most clearly defined vacuoles) was then used to choose elliptic regions of interest (ROIs) 4×4 pixels in diameter, an area that is thought to adequately compensate for any minor errors in the alignment between the FM4-64 and ratiometric images. ROIs were placed manually so as to ensure that each measurement was made in a clearly delineated region, according the schema portrayed in **Figure 6b**. For all morphometric data, a minimum of 5 images were analyzed between at least two independent viewing sessions, and an average of 92 measurements were taken for each topological domain and time point. In order to compare ratios between treatments, all measurements for each treatment were normalized by dividing by the mean outside edge ratios for that treatment (set to 1).

Table 1. Yeast strains used in this study

Strain	Genotype	Source
SEY6210	*MATα leu2-3,112 ura3-52 his3-Δ200 trp1-Δ901 lys 2-801 suc2-Δ9*	(Robinson et al., 1988)
BWY2858	SEY6210; *STE3-GFP::KanMX6*	(Prosser et al., 2010)
BWY3817	SEY6210; *MUP1-GFP::KanMX6*	(Prosser et al., 2010)
CBY26	BWY2858; *vps27::Trp1*	This Study
CBY27	BWY3817; *vps27::Trp1*	This Study
CBY28	BWY3817; *vps27::Trp1 vps4::His3MX*	This Study
BY4741	*MATa his3Δ1 leu2Δ0 met15Δ0 ura3Δ0*	(Huh et al., 2003)
Ybt1-GFP	BY4741; *YBT1-GFP::His3MX*	(Huh et al., 2003)
Fth1-GFP	BY4741; *FTH1-GFP::His3MX*	(Huh et al., 2003)
Vps33-GFP	BY4741; *VPS33-GFP::His3MX*	(Huh et al., 2003)
CBY29	Ybt1-GFP; *vps27:: KanMX6*	This Study
CBY30	Fth1-GFP; *vps27:: KanMX6*	This Study

Table 2. Primers used in this study

Name	Alias	Sequence
CBO202	*vps27*ΔF1	GCTAAGGTGAATGAGTAGTGAGTAAAGAACTAAGAACAGTCGGATCCCCGGGTTAATTAA
CBO203	*vps27*ΔR1	CTAGGTTTCTTTTTACAAATACATAGAAAAGGCTACAATAGAATTCGAGCTCGTTTAAAC
CBO204	*vps27*ΔF1*ex*	TAGAGGGTGTAAAATTATCAAGATTTTTTTTTGCTAAGGTGAATGAGTAGTG
CBO205	*vps27*ΔR1*ex*	CAAGCAATTATATATATATGTATGTATATATTTATAAGCGCTAGGTTTCTTTTTACAAAT
CBO232	*vps4*ΔF1	ATATTTATTGTATTGCTTTACGGGTACCCCCGCTGGGTGACGGATCCCCGGGTTAATTAA
CBO233	*vps4*ΔR1	AACAATGTTTCTAAGTAAAGGGAAGAGTTAACTGTCCTCTGAATTCGAGCTCGTTTAAAC
CBO234	*vps4*ΔF1*ex*	TGGTTGTTCTTTCTGTACATCTATTTATTCTTGCTTGATGATATTTATTGTATTGCTTTA
CBO235	*vps4*ΔR1*ex*	TTAGAATTGATAATGCTAGGGTATCCAATAATGAGAACAGAACAATGTTTCTAAGTAAAG

RESULTS

We hypothesize that the vacuole fusion degradation pathway can serve two purposes within cells: (1) to sort and degrade resident IMPs on vacuole membranes, and (2) to complement the MVB pathway by degrading internalized surface IMPs that mislocalize to the vacuole membrane. To prove this hypothesis, I first identified candidate cargoes, and demonstrated their localization within either pathway (i.e. on the vacuole surface for resident biosynthetic cargoes, or within the endocytic pathway for MVB cargoes). Subsequently, I demonstrated, both qualitatively and quantitatively, the active sorting of two resident vacuole cargoes, Fth1 and Ybt1. Finally, I provided evidence showing that when a known MVB cargo (Mup1) mislocalizes to the vacuole membrane, it is internalized as a result of homotypic vacuole fusion.

Identification of biosynthetic cargoes on the vacuole

Initially I sought to identify IMPs that are exclusive residents of the vacuole membrane, meaning they would follow the Golgi-to-vacuole, or AP-3 pathway (Cowles et al., 1997; Stepp et al., 1997; Burd et al., 1998), and *not* undergo endocytic trafficking (Piper et al., 1995) through the CPY pathway (Conibear and Stevens, 1998). We reasoned that the MVB pathway could never sort and degrade a vacuolar IMP that eschews the endosome, making these types of biosynthetic cargoes likely candidates for our proposed novel pathway. Accordingly, IMP candidates were selected based on three criteria: (1) the protein must possess a 'vacuole component' gene ontology (GO) classification within the *Saccharomyces* Genome Database (SGD; www.yeastgenome.org), (2) the protein must be classified as a vacuolar transporter within the Yeast Transport Protein database (YTPdb; http://homes.esat.kuleuven.be/~sbrohee/ytpdb/; Brohee et al., 2010), and (3) a GFP-

tagged variant of the protein must localize to the vacuole membrane and *not* that of the late endosome (which, in a fluorescence micrograph, is typically seen as a small puncta proximal to the vacuole), as determined from an image collection of 4156 GFP-tagged *S. cerevisiae* proteins, of which 60 were found to reside within the vacuolar membrane (Huh et al., 2003). After cross-referencing the lists procured from the aforementioned databases, I ended up with a short list of candidates, shown in **Table 3**. I then visually inspected the online micrographs (http://yeastgfp.yeastgenome.org) from Huh et al. (2003) for each listed item in order to gauge their relative GFP fluorescence, whereby the brightest cargoes were to be tested first in order to accommodate further analysis.

Ybt1 and Fth1 are exclusive residents of the vacuole membrane

As a result of pre-screening the online images for adequate fluorescence intensity, Fth1-GFP and Ybt1-GFP were chosen as the best candidates for further analysis, which would entail using epifluorescence microscopy to demonstrate their sorting either into, or out of, the contact zone during homotypic vacuole fusion. Before I could proceed however, it was necessary to establish these cargoes as exclusive residents of the vacuole membrane that are not processed by the MVB pathway for degradation.

In order to determine that Fth1 and Ybt1 indeed avoid the endosome, I knocked out the ESCRT-0 gene VPS27 from their respective GFP-tagged strains (Huh et al., 2003). Vps27 serves to coordinate MVB degradation by simultaneously recruiting ubiquitylated cargoes and the ESCRT-I complex to the site of ILV formation on the endosome (Katzmann et al., 2003). Its presence is thus required for trafficking of ubiquitylated MVB cargoes such as the a-factor pheromone receptor Ste3p (MacDonald et al., 2012a), whereby the deletion of VPS27 causes Ste3 to abberantly accumulate on the

surface of an enlarged late endosome structure called the class E compartment (Raymond et al., 1992), as shown in **Figure 2**. Although Ybt1-GFP and Fth1-GFP are uniformly distributed on the vacuole membrane *in vivo*, neither accumulates in the class E compartments of their respective *vps27*Δ deletion strains (**Figure 2**). This result indicates that both Ybt1p and Fth1p avoid the endosome en route to the vacuole, suggesting that they are trafficked through the AP-3 pathway, and thus cannot be degraded by the MVB pathway (Piper et al., 1995). The question then arises as to how these proteins are degraded, seeing as no mechanism has yet been demonstrated for exclusive residents of the vacuole membrane.

Fth1 and Ybt1 are sorted during in vitro *vacuole fusion*

After establishing that Fth1-GFP and Ybt1-GFP are viable candidates to test our hypothesis, I determined their protein localization during the *in vitro* vacuole fusion reaction, based on the approach of Wang et al. (2002). This approach was used with great success to determine protein enrichment within the vertex microdomain of docked vacuoles, but is also suitable for delineating protein localization within any of the three topological domains, be it outside, boundary, or vertex. Because our hypothesis states that cargoes sorted for degradation during vacuole fusion are included in the boundary between docked vacuoles (see **Figure 1b**), we predicted that our biosynthetic cargoes would either be enriched within, or depleted from, the boundary domain during fusion.

Figures 3, 4, and 5 reveal the distinct topological enrichments of Fh1-GFP, Ybt1-GFP, and Vps33-GFP, respectively, during *in vitro* vacuole fusion. Panel **(a)** of each figure shows the distribution of each respective protein on isolated vacuoles before the fusion reaction has begun, which is necessary as a point of comparison to the time points

shown in panel **(b)**. Notably, different time points were used for each investigated protein. Although my original intention was to follow increments (30, 60, and 90 min.) commonly used during *in vitro* fusion studies (Jun and Wickner, 2007), I prepared additional samples for early and late incubation times, knowing that the first round of fusion occurs with a half-time of < 20 min., and that fusion events persist up to 120 min. within a population of isolated vacuoles (Merz and Wickner, 2004). Accordingly, imaging revealed that each IMP cargo had its own sorting kinetics, with Fth1-GFP displaying an internalization phenotype as early as 15min., and Ybt1-GFP being most apparently excluded at 120 min., whereas my control Vps33-GFP showed vertex enrichment at all time points, as expected (Wang et al., 2002). Each protein is discussed in turn below.

The displacement of Fth1-GFP from the outside membranes to the boundary membranes during homotypic vacuole fusion is shown in **Figure 3**. Prior to *in vitro* fusion – which starts with incubation at 27˚C in the presence of ATP (Haas et al., 1994) – Fth1-GFP is uniformly distributed within the vacuole membrane, whereas shortly after the beginning of *in vitro* fusion it is found within the boundary between docked vacuoles (15-30 min.). After 90 min., Fth1-GFP can still be found within the boundary membranes of some docked vacuoles, although it is predominantly seen as a green haze within the vacuole lumen, a phenotype that commonly denotes internalization (Prosser et al., 2010). Taken together, these results indicate that Fth1p is very quickly sorted for internalization during *in vitro* homotypic vacuole fusion.

The conservation of Ybt1-GFP within outside membranes during homotypic vacuole fusion is shown in **Figure 4**. Prior to *in vitro* fusion, Ybt1-GFP is uniformly distributed within the vacuole membrane, whereas throughout the fusion reaction it

remains within the outside membranes of docked vacuoles, and is rarely seen within the vacuole lumen (up to 120 min.). Although Ybt1-GFP can nevertheless be seen within the boundary between docked vacuoles all time points, it is unclear whether this represents genuine inclusion, or an artefactual phenotype that arises due to the spatial resolution limitation of two-dimensional microscopy (specifically in the z-plane) when viewing a three dimensional cluster of docked vacuoles. Regardless, the examples of exclusion dominate at later time points, and taken together with the dearth of lumenal GFP at all time points, indicate that Ybt1p is not internalized, and thus excluded from the contact zone of docked vacuole pairings during *in vitro* homotypic vacuole fusion.

The enrichment of Vps33-GFP within the vertex microdomain during fusion is shown in **Figure 5**. Before the start of the *in vitro* fusion reaction, Vps33-GFP is unevenly distributed on the vacuole membrane. Vps33 is a component of HOPS, and expected only to associate with sites of tethering or docking between endocytic compartments, where it interacts with Ypt7 (Seals et al., 2000), or transiently chaperones *cis*-SNARE complexes (Ungermann et al., 1998a). Whereas the localization of Vps33-GFP appears arbitrary prior to fusion, it accumulates at the vertex of membrane contact between docked vacuoles at all time points during the *in vitro* homotypic fusion reaction. This result mirrors that of Wang et al. (2002), and thus verifies my experimental results, whose validity rely on an intact vacuole fusion pathway.

Having visually established the active sorting of IMP cargoes during vacuole fusion (see exemplars in **Figure 6a**), I then quantified my results using morphometric analysis (see Wang et al. (2002)), which measures the ratio of fluorescence intensity between the FM4-64 and GFP channels for any readily distinguishable topological domain within a two-channel micrograph (see **Figure 6b**). Thus, a low ratio denotes GFP

depletion, whereas a high ratio denotes GFP enrichment. Because FM4-64 is a lipophilic dye that is evenly distributed within the vacuole membrane (Vida and Emr, 1995), it is a suitable baseline to make these types of measurements. **Figures 6c-e** provide the results for this analysis, which are summarized below.

Figure 6c shows the cumulative probability plots of measurements for Fth1-GFP, Ybt1-GFP, and Vps33-GFP derived from micrographs acquired 30 min. into the *in vitro* fusion reaction – a time point at which docking is thought to be most readily apparent (Jun and Wickner, 2007). **Figure 6d** shows the mean values for the same measurements. This analysis confirms Fth1-GFP enrichment of the boundary, Ybt1-GFP exclusion from the same, and Vps33-GFP enrichment of the vertex. However, there are two potential sources of bias: (1) because the boundary and vertex domains are proximal (especially if the contact zone is relatively small), measurements of either class may overlap, and (2) because exclusion of cargoes from the contact zone could entail the accumulation of IMP cargoes along the vertex (see **Figure 1b**), measurements from within this domain may be skewed for any cargo showing an exclusion phenotype. These considerations (along with the aforementioned spatial resolution limits of two-dimensional microscopy) explain why Ybt1-GFP fluorescence may not be depleted within the boundary domain at 30 min. (as expected), but instead shows little variation between the mean values for any of the three domains (**Figure 6d**). It is thus necessary to look at the distribution of measurements within the boundary domain for this protein (**Figure 6c**, top), which show a skewed distribution toward lower ratios. Apparent discrepancies with Fth1-GFP and Vps33-GFP (which show simultaneous GFP enrichment of the vertex and boundary domains) are also explained by this rationale, especially given that Wang et al. (2002) obtained similar results for Vps33p. Finally, **Figure 6e** shows the mean outside ratios

after 90 min. into the *in vitro* homotypic fusion reaction, relative to those measured before the reaction has begun. As expected, Fth1p shows significant depletion from this domain, confirming that it is sorted into the boundary and internalized, whereas Ybt1-GFP and Vps33-GFP show relatively minimal depletion, indicating that they are spared.

All together, these results provide the first evidence of biosynthetic IMP sorting within the homotypic vacuole fusion pathway, which can henceforth be considered a selective IMP degradation pathway.

Mislocalized Mup1 is internalized during in vitro *vacuole fusion*

Given that cells lacking VPS27 effectively lack a functional MVB pathway but still remain viable, and that cargoes utilizing the MVB pathway have already been shown to colonize the vacuole membrane within a MVB-deficient genetic background (Luhtala and Odorizzi, 2004), we hypothesized that mislocalized MVB cargoes could be degraded as a result of homotypic vacuole fusion. That is, IMP cargoes undergoing endocytic trafficking due to their ubiquitylation end up stuck on the limiting membrane of class E compartments (Raymond et al., 1992), and through many successive endosome-vacuole fusion events, colonize the vacuole membrane, making them viable candidates for our proposed mechanism. We set out to demonstrate this effect using a Mup1-GFP expressing strain that was generously provided by Beverly Wendland (Johns Hopkins University; Baltimore, MD, USA). Mup1 is a high affinity methionine permease (Kosugi et al., 2001) whose maintenance on the plasma membrane is starvation-dependent (Prosser et al., 2010). Under rich media growth, it is ubiquitylated and traffics to the endosome, where it is packaged into ILVs as an MVB cargo, and eventually deposited into the vacuole lumen for degradation (Jones et al., 2012; MacDonald et al., 2012a).

To induce Mup1 colonization of the vacuole membrane, I created both single *vps27*Δ, and double *vps27*Δ*vps4*Δ mutants from our Mup1-GFP strain. Both mutant strains displayed visually detectable Mup1-GFP on the vacuole membrane (**Figure 7**), albeit only within a subpopulation of cells. We reasoned that because *vps27*Δ*vps4*Δ double mutants cannot sort IMP cargoes *or* make ILVs, they may have more IMP cargoes on the surface of their class E compartments, allowing for more spillover onto the vacuole membrane. However, there was little discernable difference between these strains with respect to vacuole localization, and because the *vps27*Δ*vps4*Δ double mutants had a more severe class E phenotype (which made it difficult to discern between vacuoles and class E compartments), we chose the *vps27*Δ single deletion strain for further analysis.

Although only a fraction of isolated vacuoles from *vps27*Δ Mup1-GFP expressing cells displayed any GFP fluorescence on the vacuole membrane (**Figure 8a**), we reasoned that a population of vacuoles could still provide evidence of cargo internalization. Accordingly, **Figure 8b** shows that as *in vitro* vacuole fusion proceeds, a subset of vacuoles accumulate GFP fluorescence in their lumen, which, similar to Fth1-GFP, denotes internalization. Two additional observations support this notion. First, certain docked vacuole clusters display boundary enrichment of Mup1-GFP (see 90 min. images in **Figure 8**). Second, only relatively large vacuoles (i.e. fusion products) were seen to contain intralumenal GFP, and the appearance of these was far greater at late time points, which, again similar to Fth1-GFP, indicates that Mup1-GFP internalization occurred as a function of homotypic vacuole fusion.

Performing morphometric analysis proved difficult for micrographs obtained from Mup1-GFP*vps27*Δ cells. Large, brightly fluorescing class E compartments always

accompany the vacuoles isolated from this strain, and were often found directly adjacent to vacuoles within *in vitro* fusion micrographs, which served to confound the manual placement of ROIs (see Materials & Methods), and thus gave uninterpretable data. Regardless, the micrographs presented here support the hypothesis that homotypic vacuole fusion can serve to internalize MVB cargoes when this pathway is defective, and thus provide an explanation for why class E mutants remain viable.

Table 3. Short list of biosynthetic IMP cargoes suitable for analysis

Standard Name	Systematic Name	SGD Description (www.yeastgenome.org)
Bpt1	YLL015W	ABC type glutathione S-conjugate transporter
Cot1	YOR316C	Zinc importer; Zrc1 paralog
Fth1	YBR207W	Putative high affinity iron transporter
Mch1	YDL054C	Putative monocarboxylate permease
Ncr1	YPL006W	Mammalian Npc1 orthologue; involved in sphingolipid metabolism
Pmc1	YGL006W	Ca^{2+} ATPase; regulates Ca^{2+} efflux
Ybt1	YLL048C	ABC type bile acid transporter; regulates Ca^{2+} efflux
Ycf1	YDR135C	ABC type glutathione S-conjugate transporter
Ypq1	YOL092W	Putative cationic amino acid exporter
Ypq2	YDR352W	Putative cationic amino acid exporter; Ypq1 paralog
Zrc1	YMR243C	Zinc importer

Figure 2. Resident vacuole IMPs eschew the endosome en route to the vacuole

Live cell imaging of GFP-tagged IMP cargo strains and their *vps27*Δ counterparts show that Fth1-GFP and Ybt1-GFP traffic directly to the vacuole membrane, whereas Ste3-GFP accumulates in the class E compartment of vps27Δ cells, indicating that it traffics through the MVB pathway for its degradation. Distinguishing features are enlarged (2×) in the last column. For all *vps27*Δ strains, class E compartments are indicated with purple arrows in the FM4-64 channel.

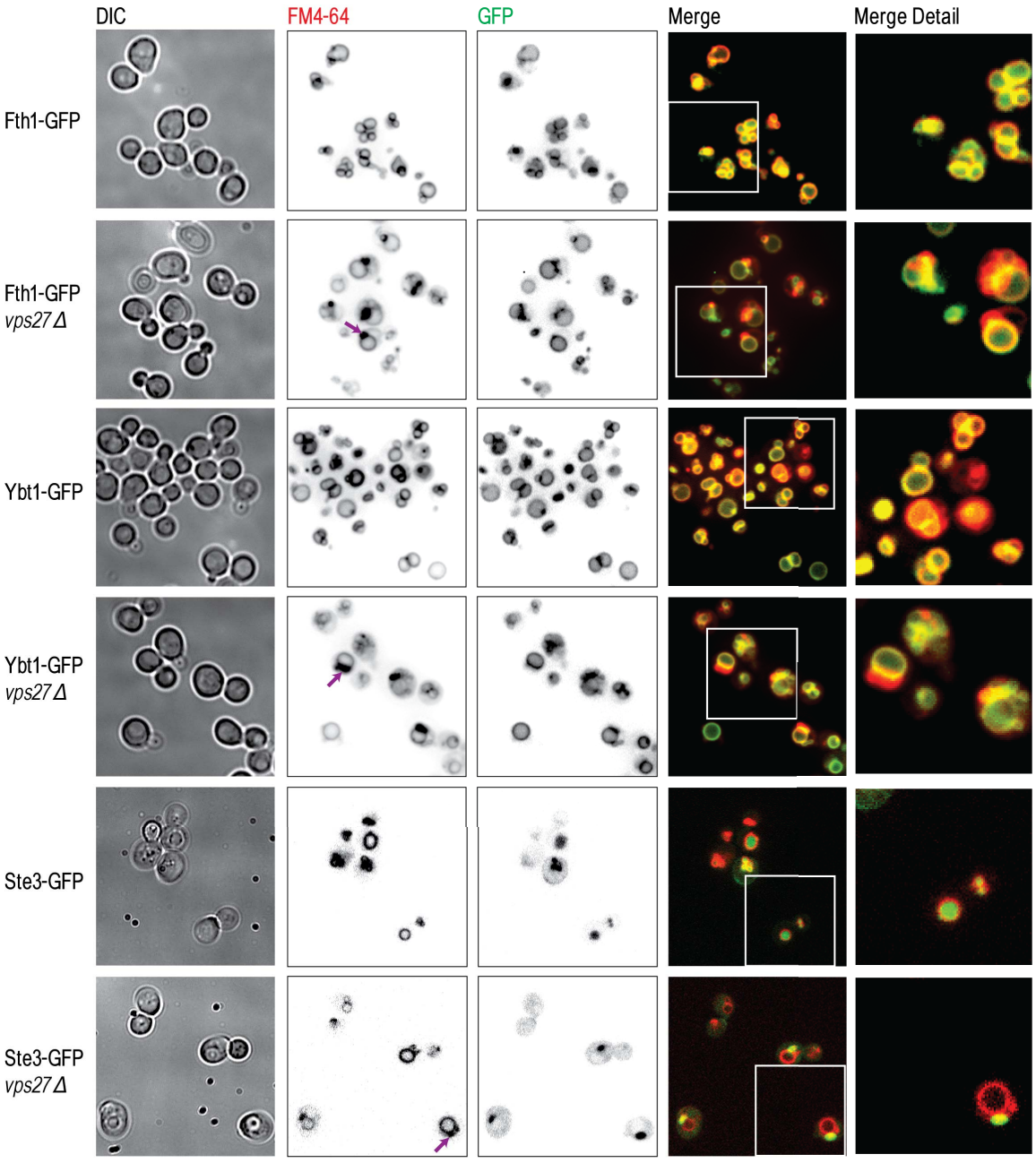
DIC
FM4-64
GFP
Merge
Merge Detail
Fth1-GFP
Fth1-GFP
vps27Δ
Ybt1-GFP
Ybt1-GFP
vps27Δ
Ste3-GFP
Ste3-GFP
vps27Δ

Figure 3. Boundary inclusion of Fth1-GFP during *in vitro* vacuole fusion

(a) Vacuoles isolated from Fth1-GFP expressing cells show that Fth1-GFP is uniformly distributed on the vacuole membrane prior to the start of *in vitro* fusion. **(b)** Vacuoles undergoing *in vitro* fusion (+ATP, +salts, incubation at 27˚C, see Materials & Methods) demonstrate the active sorting of Fth1-GFP into the boundary between docked vacuoles at 15, 30, and 90 min. Purple arrows indicate regions where boundary inclusion is especially apparent.

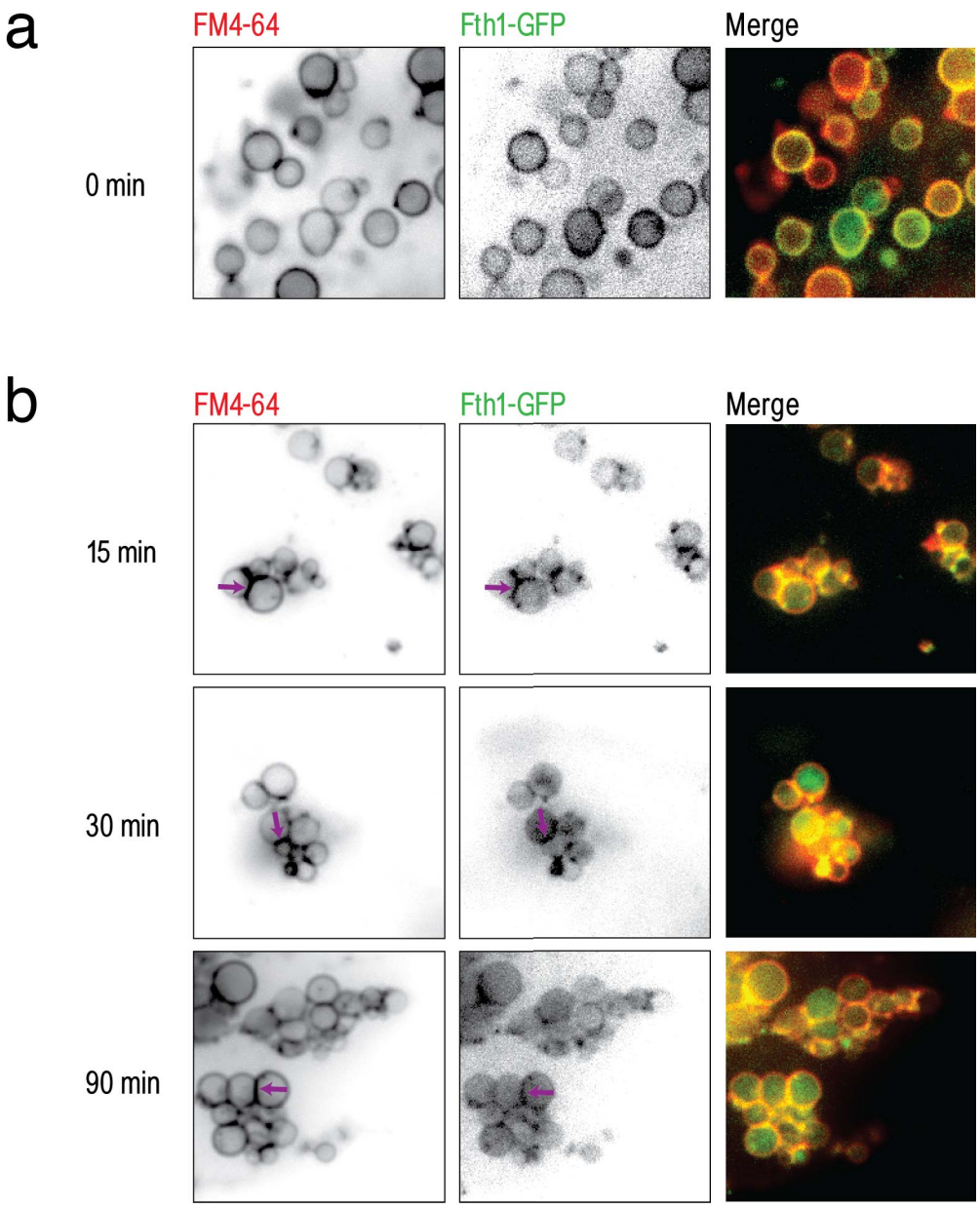
a
FM4-64
Fth1-GFP
Merge
0 min
b
FM4-64
Fth1-GFP
Merge
15 min
30 min
90 min

Figure 4. Boundary exclusion of Ybt1-GFP during *in vitro* vacuole fusion

(a) Vacuoles isolated from Ybt1-GFP expressing cells show that Ybt1-GFP is uniformly distributed on the vacuole membrane prior to the start of *in vitro* fusion. **(b)** Vacuoles undergoing *in vitro* fusion (+ATP, +salts, incubation at 27˚C, see Materials & Methods) demonstrate the active sorting of Ybt1-GFP out of the boundary between docked vacuoles at 30, 90, and 120 min. Purple arrows indicate regions where boundary exclusion is especially apparent.

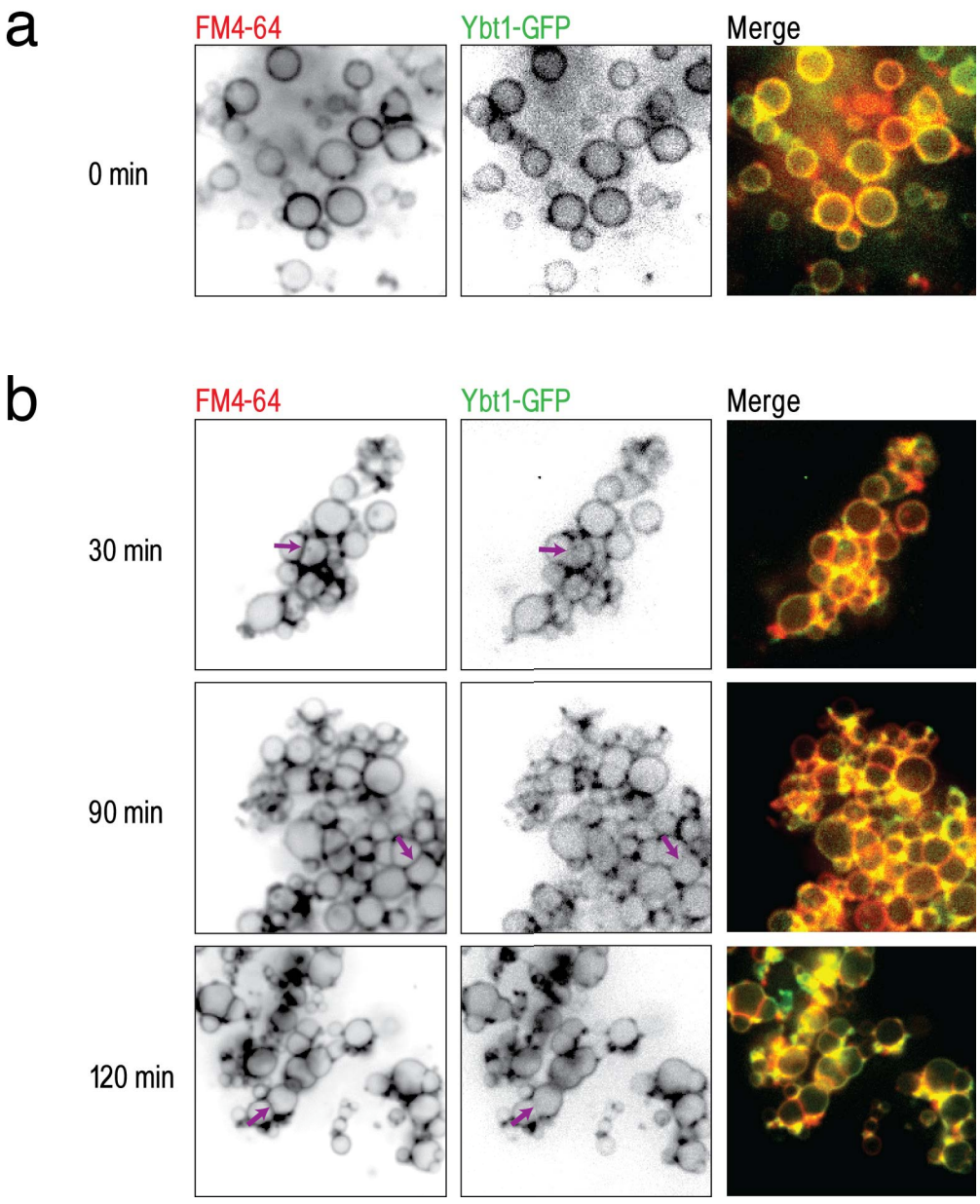
a
FM4-64
Ybt1-GFP
Merge
0 min
b
FM4-64
Ybt1-GFP
Merge
30 min
90 min
120 min

Figure 5. Vertex enrichment of Vps33-GFP during *in vitro* vacuole fusion

(a) Vacuoles isolated from Vps33-GFP expressing cells show that Vps33-GFP is arbitrarily distributed on the vacuole membrane prior to the start of *in vitro* fusion. **(b)** Vacuoles undergoing *in vitro* fusion (+ATP, +salts, incubation at 27˚C, see Materials & Methods) demonstrate the enrichment of Vps33-GFP within the vertex microdomain between docked vacuoles at 30, 60, and 90 min. Purple arrows indicate regions where vertex enrichment is especially apparent.

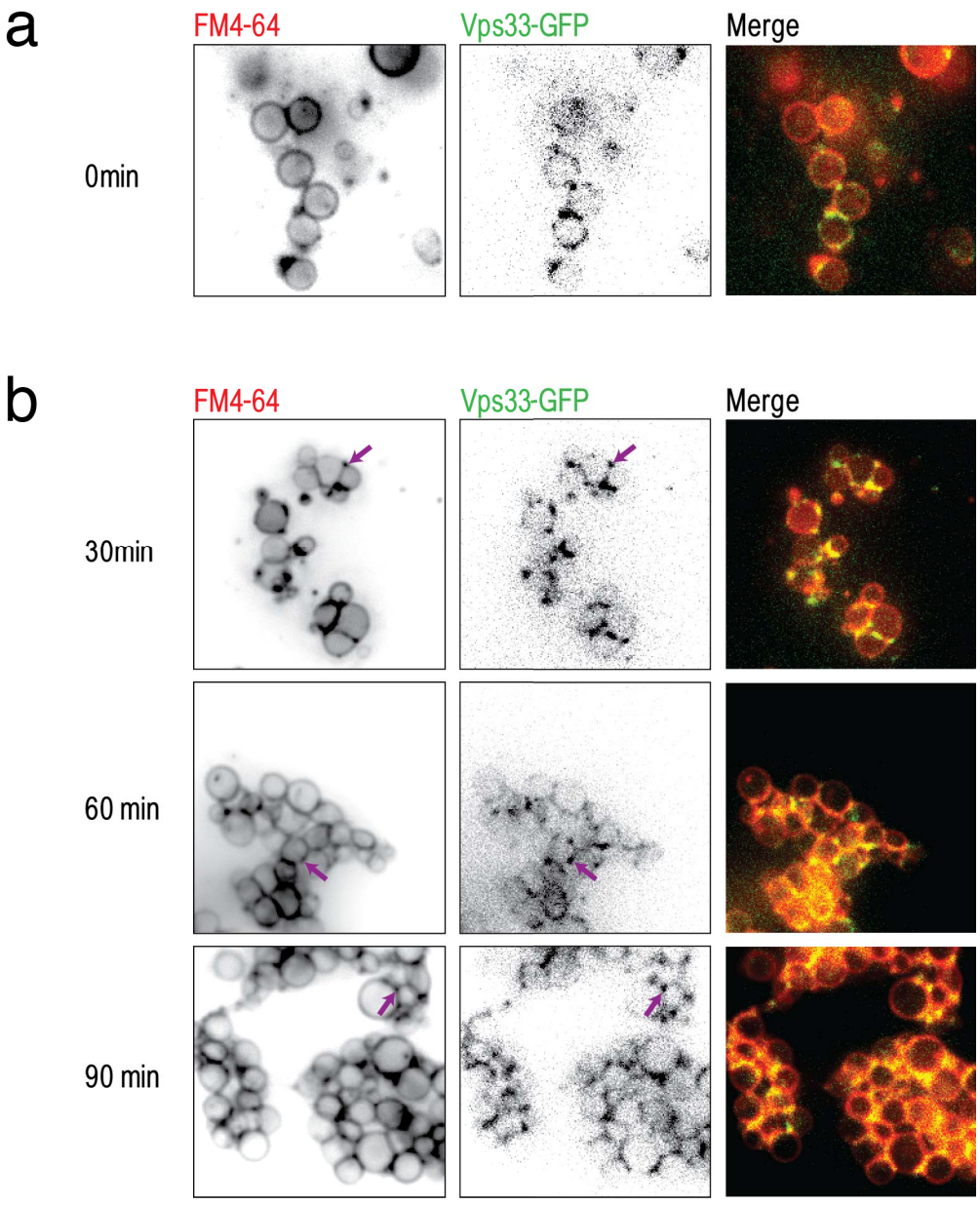
a
FM4-64
Vps33-GFP
Merge
0min
b
FM4-64
Vps33-GFP
Merge
30min
60 min
90 min

Figure 6. Morphometric analysis of protein localization on docked vacuole clusters

(a) Exemplar micrographs showing boundary inclusion, boundary exclusion, and vertex enrichment at 30 min., of Fth1-GFP, Ybt1-GFP, and Vps33-GFP, respectively. **(b)** Schematic depicting where ROIs were placed within a cluster of vacuoles during morphometric analysis (see Materials & Methods). **(c)** Mean ratio (± SEM) values at 30 min. for (O)utside, (B)oundary, and (V)ertex topological domains. **(d)** Cumulative distribution plots show the range of ratio values obtained for each topological domain after 30 min. The intersection of each profile with the 50^{th} percentile line indicates the median value. For each treatment, an average of 95 ratio measurements were taken for each topological domain, from at least five micrographs spanning at least two independent experiments. **(e)** Mean outside ratio (± SEM) values for each protein after 90 min., relative to their mean outside ratio values at 0 min., indicating the depletion of each respective protein from outside membranes. An average of 96 and 86 outside ratio measurements were made for each protein for the 90 min. and 0 min. time points, respectively. Measurements were taken from at least five micrographs spanning at least two independent experiments.

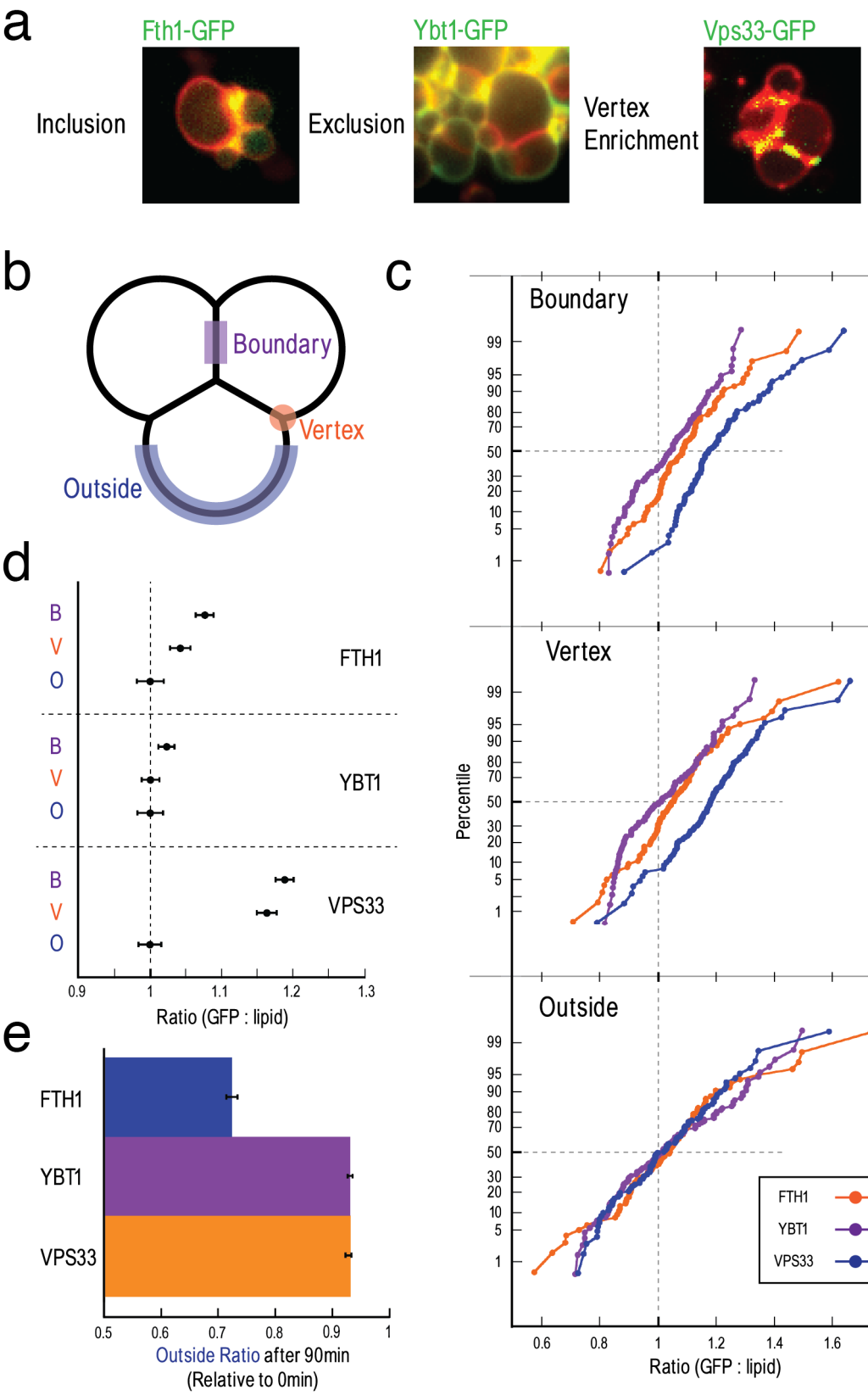
a
Fth1-GFP
Ybt1-GFP
Vps33-GFP
Inclusion
Exclusion
Vertex
Enrichment
b
Boundary
Vertex
Outside
c
Boundary
Vertex
Outside
Percentile
99
95
90
80
70
50
30
20
10
5
1
0.6
0.8
1
1.2
1.4
1.6
1.8
Ratio (GFP : lipid)
FTH1
YBT1
VPS33
d
B
V
O
FTH1
YBT1
VPS33
0.9
1
1.1
1.2
1.3
Ratio (GFP : lipid)
e
FTH1
YBT1
VPS33
0.5
0.6
0.7
0.8
0.9
1
Outside Ratio after 90min
(Relative to 0min)

Figure 7. Mup1-GFP colonizes the vacuole membrane in MVB mutant cells

Live cell imaging of *vps27*Δ or *vps27*Δ*vps4*Δ Mup1-GFP expressing cells shows that in either genetic background, Mup1-GFP can traffic to the vacuole limiting membrane, rather than the vacuole lumen, where it is normally deposited for its degradation. Distinguishing features are enlarged (2×) in the last column. Purple arrows indicate vacuoles where Mup1-GFP has reached the vacuole membrane.

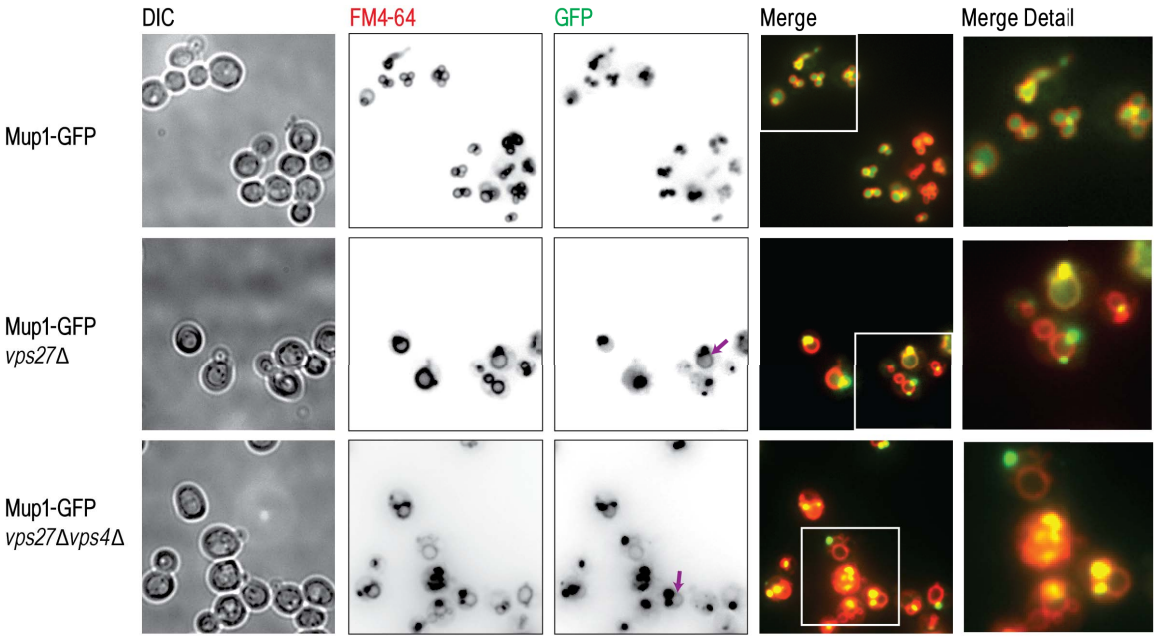
DIC
FM4-64
GFP
Merge
Merge Detail
Mup1-GFP
Mup1-GFP
vps27Δ
Mup1-GFP
vps27Δvps4Δ

Figure 8. Internalization of Mup1-GFP during *in vitro* vacuole fusion

(a) Vacuoles isolated from Mup1-GFP expressing yeast cells show that Mup1-GFP is uniformly distributed on the vacuole membrane of a subset of the total vacuole population prior to the start of *in vitro* fusion. **(b)** Vacuoles undergoing *in vitro* fusion (+ATP, +salts, incubation at 27˚C, see Materials & Methods) demonstrate the internalization of Mup1-GFP at 30 and 90 min. The purple arrow at 90 min. indicates the possible enrichment of Mup1-GFP in the boundary between docked vacuoles.

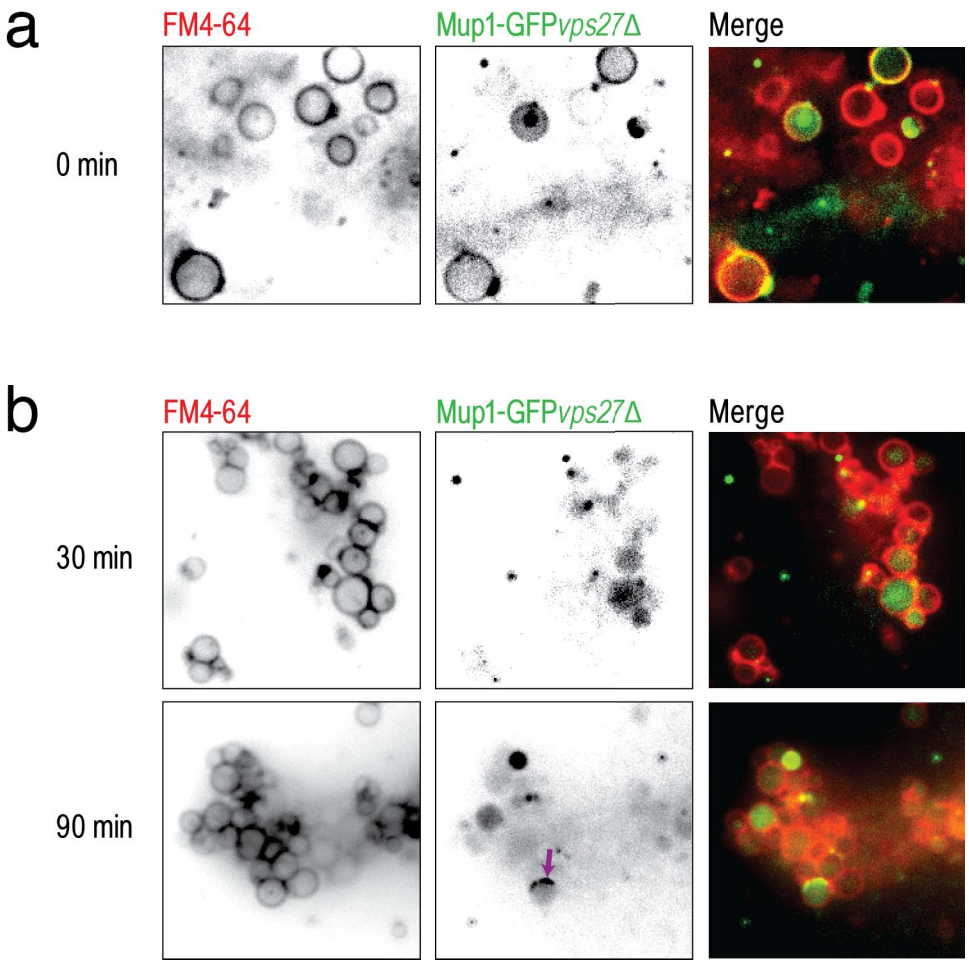
a
FM4-64
Mup1-GFPvps27Δ
Merge
0 min
b
FM4-64
Mup1-GFPvps27Δ
Merge
30 min
90 min

DISCUSSION

Our proposed selective IMP degradation pathway entails that cargoes are sorted by the vacuole fusion machinery into the contact zone between docked vacuoles (**Figure 1b**), which becomes internalized as a result of fusion (Wang et al., 2002). Upon internalization, these IMPs would ultimately be degraded by the myriad catabolic enzymes within the vacuole lumen (Sarry et al., 2007) that normally degrade biological membranes and proteins (Li and Kane, 2009). In order to demonstrate this mechanism, I used epifluorescence microscopy to show that two resident vacuole IMPs – Fth1 and Ybt1 – are sorted into, or out of, respectively, the contact zone between docked vacuoles, or the lumen of vacuoles that have undergone previous rounds of fusion. Additionally, I used similar methods to show that Mup1 – a known MVB cargo – can colonize the vacuole membrane when the MVB pathway is abrogated, and subsequently enter the vacuole lumen during homotypic vacuole fusion. Although these results fail to provide a mechanistic explanation for IMP sorting during vacuole fusion, they demonstrate the existence of this phenomenon, and thus illustrate the exquisite efficiency of IMP degradation, where distinct pathways can nevertheless complement one another.

Implications

Demonstrating that Fth1, Ybt1, and Mup1 are sorted during homotypic vacuole fusion provides valuable and distinct insights as to their function and turnover in *S. cerevisiae*. Each protein is addressed separately below.

Fth1 is a Ftr1 homologue that associates with Fet5, a Fet3 homologue, in order to coordinate the efflux of Fe^{2+} stores from the vacuole lumen into the cytosol (Urbanowski and Piper, 1999). Analogous to Fth1/Fet5 on the vacuole, Ftr1 is a high-affinity Fe^{3+}-

transporter that associates with Fet3 (an iron oxidase), in order to coordinate the transport of extracellular Fe^{2+} across the plasma membrane into the cell (Askwith et al., 1994; Eide, 1998). Previously, it was shown that high levels of extracellular iron lead to the ubiquitylation of Ftr1 (but not Fet3), which targets Ftr1/Fet3 for degradation through the MVB pathway (Felice et al., 2005). Understanding the Ftr1/Fet3 response to fluctuating iron levels has been instrumental in the development of both the MVB pathway (Felice et al., 2005; Strochlic et al., 2008; Prosser et al., 2010), as well as Tor1-mediated nutrient sensing pathways (Jones et al., 2012), so the opportunity to describe a similar mechanism acting at the vacuole is enticing. However, discovering the mechanism of Fth1 (and by extension, Fet5) turnover is only the first step. Future studies should therefore entail repeating our protein sorting analysis using vacuoles isolated from Fth1-GFP and/or Fet5-GFP expressing cells grown in iron-reduced media. This could provide the key to showing Fth1 exclusion from the contact zone during homotypic vacuole fusion, and thus provide a complementary explanation for nutrient signaling that regulates vacuolar – rather than plasma membrane – IMP turnover.

Ybt1 is one of five class-C ABC-transporters that are found on the yeast vacuole, and as such, is thought to mediate the transport of toxic glutathione-conjugated substrates across the vacuolar membrane, either to metabolize them, or more likely, to sequester them from their cytosolic targets (Paumi et al., 2009). Although the ABC-transporter family is large and functionally diverse, it is worth noting that Bpt1 and Ycf1 – the most closely related ABC-C transporters to Ybt1 (Paumi et al., 2009) – are also on our short list of candidate IMPs to be sorted and degraded through homotypic vacuole fusion (see **Table 3**). Accordingly, Ycf1 has also been shown to eschew the endosome en route to the vacuole (Wemmie and Moye-Rowley, 1997). Ybt1, Ycf1, and Bpt1 are yeast

orthologues to the human ABC-C transporter MRP1, which – due to its parallel function of transporting various endogenous and xenobiotic anionic substances – is a widely cited target in studies pertaining to drug resistance, as well as numerous disease pathophysiologies (He et al., 2011; Keppler, 2011). It is therefore necessary to uncover the degradation mechanism for the yeast orthologues in order to establish yeast models that could recapitulate the human cellular phenotypes that arise from aberrant trafficking or turnover of MRP1, for which little mechanistic detail is currently known (Porcelli et al., 2009).

Mup1p is a cell surface methionine permease and known cargo of the MVB pathway, which is responsible for degrading IMP cargoes that have been endocytosed upon their ubiquitylation (MacDonald et al., 2012a). By showing that the fusion pathway can complement the MVB pathway, I have provided a solution for the problem as to why cells remain viable once their primary mechanism of IMP degradation has been abrogated. Apart from addressing this question however, my results also point to an explanation for how the fusion machinery can sort IMPs. Because MVB cargoes must be ubiquitylated to get sorted and packaged into ILVs, it is possible that the fusion machinery also sorts IMP cargoes based on their ubiquitylation status. This hypothesis is supported by the following three observations. First, endosomal cargoes are ubiquitylated by the cytosolic Ub-ligase Rsp5 (Lauwers et al., 2010), which is recruited to endosomal membranes by the endosomal IMP Sna3 (MacDonald et al., 2012b), whose homolog of unknown function, Sna4, resides within the vacuole membrane (http://yeastgfp.yeastgenome.org; Huh et al., (2003)). Second, both Fth1 and Ybt1, which I have shown to be sorted during homotypic vacuole fusion (**Figures 3 and 4**, respectively), interact with Sna4, and Sna4 interacts with Rsp5p (http://thebiogrid.org;

Stark et al., 2006), hinting at a possible mechanism of vacuolar IMP ubiquitylation. Third, Ste6, a cell-surface ABC-transporter responsible for the release of the a-factor mating pheromone, is endocytosed and degraded through the MVB pathway as a result of its ubiquitylation (Kelm et al., 2004), demonstrating that ABC-transporters (like Ybt1) can be sorted based on their ubiquitylation, and thus could also (like Mup1), be internalized as a result of homotypic vacuole fusion.

Therefore, to describe the mechanism of IMP sorting that is intrinsic to homotypic vacuole fusion, future studies should investigate the possibility that the fusion machinery sorts IMP cargoes based on their ubiquitylation status.

Can HOPS sort ubiquitylated IMPs for degradation during homotypic vacuole fusion?

Given the possibility that ubiquitin is the sorting-signal that targets vacuolar IMPs for degradation, it is necessary to also ask, what performs the task of sorting? Three observations indicate that HOPS could sort Ub-tagged IMPs into the contact zone during homotypic vacuole fusion. First, HOPS concentrates within the vertex microdomain, whose highly organized structure (Wang et al., 2002; Fratti et al., 2004) likely prevents passive IMP movement from outside to boundary membranes. Second, Vps11, Vps18, and Vps39 contain partial RING (really interesting new gene) domains (Nickerson et al., 2009), which may combine within the HOPS superstructure to form an intact and functional RING domain, a Ub-interacting domain commonly found within Ub-ligases (Budhidarmo et al., 2012). Third, when the partial RING domain of Vps39 is removed, HOPS continues to drive vacuole fusion (Plemel et al., 2011), suggesting this domain is expendable with respect to coordinating vacuole fusion, but also begging the question as to why it is present.

This last observation reveals an important limitation on the investigation of the potential role for HOPS in IMP sorting, namely that deleting the proposed sorting domains from HOPS subunits may also affect vacuole fusion itself. The consequences of this problem are seen when the partial RING domains are deleted from Vps11 or Vps18, yielding morphological defects in cells that denote impaired vacuole fusion (Plemel et al., 2011). This result is not surprising however, given that Vps11 and Vps18 compose the core of the HOPS holocomplex, and are essential for its integrity (Bröcker et al., 2012). Uncoupling fusion from sorting thus represents a daunting (yet crucial) obstacle to overcome if HOPS is to be characterized with respect to the latter. However, an attractive approach was recently developed by Stringer and Piper (2011), who engineered the catalytic domain of the yeast deubiquitinase Ubp7 into a protein tag (termed the DUb tag) whose attachment effectively turns its cognate protein into a deubiquitinase enzyme. By attaching this DUb tag to a HOPS subunit (in a way that does not affect vacuole fusion), it would be possible to control the ubiquitylation status of any proteins that approach HOPS within the vertex microdomain, which according to our hypothesis and analysis, would yield only IMP boundary exclusion during vacuole fusion. Conversely, directly attaching a ubiquitin moiety to IMP cargoes of interest would necessitate their inclusion in the boundary domain during vacuole fusion (as deubiquitinase enzymes cannot break peptide bonds), thus providing the reciprocal control for these types of experiments.

Regardless of the chosen investigative approach, HOPS is an excellent candidate to provide a mechanistic explanation of protein sorting within the vertex microdomain during the homotypic vacuole fusion pathway, and should thus be the focus of future research into the same.

Concluding Remarks

Although this work only represents a first step toward fully elucidating the selective IMP degradation pathway intrinsic to homotypic vacuole fusion, it definitively proves its existence, and thus represents a major addition to the field of yeast cellular biology. As discussed above, this mechanism has tremendous potential to address unanswered questions with respect to vacuolar IMP trafficking and turnover. Additionally, should the role of HOPS be confirmed, its expanded functional repertoire would necessitate the re-evaluation of many previous studies, especially as HOPS is evolutionarily conserved in all eukaryotes (Zlatic et al., 2011), and its dysfunction has now been implicated in various human disease etiologies, including the mechanism of invasion of the Ebola virus (Carette et al., 2011), the efficient clearance of toxic α-synuclein protein species linked with Parkinson's disorder (Harrington et al., 2012), or the deficiencies in pigment trafficking associated with Hermansky-Pudlak syndrome (Schonthaler et al., 2008).

REFERENCES

Askwith, C., D. Eide, A. Van Ho, P.S. Bernard, L. Li, S. Davis-Kaplan, D.M. Sipe, and J. Kaplan. 1994. The FET3 gene of S. cerevisiae encodes a multicopper oxidase required for ferrous iron uptake. *Cell*. 76:403-410.

Babst, M., D.J. Katzmann, E.J. Estepa-Sabal, T. Meerloo, and S.D. Emr. 2002a. Escrt-III: an endosome-associated heterooligomeric protein complex required for mvb sorting. *Developmental cell*. 3:271-282.

Babst, M., D.J. Katzmann, W.B. Snyder, B. Wendland, and S.D. Emr. 2002b. Endosome-associated complex, ESCRT-II, recruits transport machinery for protein sorting at the multivesicular body. *Developmental cell*. 3:283-289.

Babst, M., T.K. Sato, L.M. Banta, and S.D. Emr. 1997. Endosomal transport function in yeast requires a novel AAA-type ATPase, Vps4p. *The EMBO journal*. 16:1820-1831.

Boeddinghaus, C., A.J. Merz, R. Laage, and C. Ungermann. 2002. A cycle of Vam7p release from and PtdIns 3-P-dependent rebinding to the yeast vacuole is required for homotypic vacuole fusion. *The Journal of cell biology*. 157:79-89.

Bowers, K., S.C. Piper, M.A. Edeling, S.R. Gray, D.J. Owen, P.J. Lehner, and J.P. Luzio. 2006. Degradation of endocytosed epidermal growth factor and virally ubiquitinated major histocompatibility complex class I is independent of mammalian ESCRTII. *The Journal of biological chemistry*. 281:5094-5105.

Bradford, M.M. 1976. A rapid and sensitive method for the quantitation of microgram quantities of protein utilizing the principle of protein-dye binding. *Analytical biochemistry*. 72:248-254.

Brett, C.L., R.L. Plemel, B.T. Lobingier, M. Vignali, S. Fields, and A.J. Merz. 2008. Efficient termination of vacuolar Rab GTPase signaling requires coordinated action by a GAP and a protein kinase. *The Journal of cell biology*. 182:1141-1151.

Bröcker, C., S. Engelbrecht-Vandre, and C. Ungermann. 2010. Multisubunit tethering complexes and their role in membrane fusion. *Current biology : CB*. 20:R943-952.

Bröcker, C., A. Kuhlee, C. Gatsogiannis, H.J. Balderhaar, C. Honscher, S. Engelbrecht-Vandre, C. Ungermann, and S. Raunser. 2012. Molecular architecture of the multisubunit homotypic fusion and vacuole protein sorting (HOPS) tethering complex. *Proceedings of the National Academy of Sciences of the United States of America*. 109:1991-1996.

Brohee, S., R. Barriot, Y. Moreau, and B. Andre. 2010. YTPdb: a wiki database of yeast membrane transporters. *Biochimica et biophysica acta*. 1798:1908-1912.

Budhidarmo, R., Y. Nakatani, and C.L. Day. 2012. RINGs hold the key to ubiquitin transfer. *Trends in Biochemical Sciences*. 2:58-65.

Burd, C.G., M. Babst, and S.D. Emr. 1998. Novel pathways, membrane coats and PI kinase regulation in yeast lysosomal trafficking. *Seminars in cell & developmental biology*. 9:527-533.

Calero, M., C.Z. Chen, W. Zhu, N. Winand, K.A. Havas, P.M. Gilbert, C.G. Burd, and R.N. Collins. 2003. Dual prenylation is required for Rab protein localization and function. *Molecular biology of the cell*. 14:1852-1867.

Carette, J.E., M. Raaben, A.C. Wong, A.S. Herbert, G. Obernosterer, N. Mulherkar, A.I. Kuehne, P.J. Kranzusch, A.M. Griffin, G. Ruthel, P. Dal Cin, J.M. Dye, S.P. Whelan, K. Chandran, and T.R. Brummelkamp. 2011. Ebola virus entry requires the cholesterol transporter Niemann-Pick C1. *Nature*. 477:340-343.

Chomczynski, P., and N. Sacchi. 1987. Single-step method of RNA isolation by acid guanidinium thiocyanate-phenol-chloroform extraction. *Analytical biochemistry*. 162:156-159.

Conibear, E., and T.H. Stevens. 1998. Multiple sorting pathways between the late Golgi and the vacuole in yeast. *Biochimica et biophysica acta*. 1404:211-230.

Cowles, C.R., W.B. Snyder, C.G. Burd, and S.D. Emr. 1997. Novel Golgi to vacuole delivery pathway in yeast: identification of a sorting determinant and required transport component. *The EMBO journal*. 16:2769-2782.

Eide, D.J. 1998. The molecular biology of metal ion transport in Saccharomyces cerevisiae. *Annual review of nutrition*. 18:441-469.

Eitzen, G., E. Will, D. Gallwitz, A. Haas, and W. Wickner. 2000. Sequential action of two GTPases to promote vacuole docking and fusion. *The EMBO journal*. 19:6713-6720.

Felice, M.R., I. De Domenico, L. Li, D.M. Ward, B. Bartok, G. Musci, and J. Kaplan. 2005. Post-transcriptional regulation of the yeast high affinity iron transport system. *The Journal of biological chemistry*. 280:22181-22190.

Fratti, R.A., Y. Jun, A.J. Merz, N. Margolis, and W. Wickner. 2004. Interdependent assembly of specific regulatory lipids and membrane fusion proteins into the vertex ring domain of docked vacuoles. *The Journal of cell biology*. 167:1087-1098.

Gao, Y., S. Zorman, G. Gundersen, Z. Xi, L. Ma, G. Sirinakis, J.E. Rothman, and Y. Zhang. 2012. Single reconstituted neuronal SNARE complexes zipper in three distinct stages. *Science*. 337:1340-1343.

Haas, A., B. Conradt, and W. Wickner. 1994. G-protein ligands inhibit in vitro reactions of vacuole inheritance. *The Journal of cell biology*. 126:87-97.

Harrington, A.J., T.A. Yacoubian, S.R. Slone, K.A. Caldwell, and G.A. Caldwell. 2012. Functional analysis of VPS41-mediated neuroprotection in Caenorhabditis elegans and mammalian models of Parkinson's disease. *The Journal of neuroscience : the official journal of the Society for Neuroscience*. 32:2142-2153.

He, S.M., R. Li, J.R. Kanwar, and S.F. Zhou. 2011. Structural and functional properties of human multidrug resistance protein 1 (MRP1/ABCC1). *Current medicinal chemistry*. 18:439-481.

Henne, W.M., N.J. Buchkovich, and S.D. Emr. 2011. The ESCRT pathway. *Developmental cell*. 21:77-91.

Hickey, C.M., C. Stroupe, and W. Wickner. 2009. The major role of the Rab Ypt7p in vacuole fusion is supporting HOPS membrane association. *The Journal of biological chemistry*. 284:16118-16125.

Huh, W.K., J.V. Falvo, L.C. Gerke, A.S. Carroll, R.W. Howson, J.S. Weissman, and E.K. O'Shea. 2003. Global analysis of protein localization in budding yeast. *Nature*. 425:686-691.

Ignatev, A., S. Kravchenko, A. Rak, R.S. Goody, and O. Pylypenko. 2008. A structural model of the GDP dissociation inhibitor rab membrane extraction mechanism. *The Journal of biological chemistry*. 283:18377-18384.

Jones, C.B., E.M. Ott, J.M. Keener, M. Curtiss, V. Sandrin, and M. Babst. 2012. Regulation of membrane protein degradation by starvation-response pathways. *Traffic*. 13:468-482.

Jun, Y., R.A. Fratti, and W. Wickner. 2004. Diacylglycerol and its formation by phospholipase C regulate Rab- and SNARE-dependent yeast vacuole fusion. *The Journal of biological chemistry*. 279:53186-53195.

Jun, Y., and W. Wickner. 2007. Assays of vacuole fusion resolve the stages of docking, lipid mixing, and content mixing. *Proceedings of the National Academy of Sciences of the United States of America*. 104:13010-13015.

Kato, M., and W. Wickner. 2001. Ergosterol is required for the Sec18/ATP-dependent priming step of homotypic vacuole fusion. *The EMBO journal*. 20:4035-4040.

Katzmann, D.J., M. Babst, and S.D. Emr. 2001. Ubiquitin-dependent sorting into the multivesicular body pathway requires the function of a conserved endosomal protein sorting complex, ESCRT-I. *Cell*. 106:145-155.

Katzmann, D.J., C.J. Stefan, M. Babst, and S.D. Emr. 2003. Vps27 recruits ESCRT machinery to endosomes during MVB sorting. *The Journal of cell biology*. 162:413-423.

Kelm, K.B., G. Huyer, J.C. Huang, and S. Michaelis. 2004. The internalization of yeast Ste6p follows an ordered series of events involving phosphorylation, ubiquitination, recognition and endocytosis. *Traffic*. 5:165-180.

Keppler, D. 2011. Multidrug resistance proteins (MRPs, ABCCs): importance for pathophysiology and drug therapy. *Handbook of experimental pharmacology*:299-323.

Kosugi, A., Y. Koizumi, F. Yanagida, and S. Udaka. 2001. MUP1, high affinity methionine permease, is involved in cysteine uptake by Saccharomyces cerevisiae. *Bioscience, biotechnology, and biochemistry*. 65:728-731.

Kramer, L., and C. Ungermann. 2011. HOPS drives vacuole fusion by binding the vacuolar SNARE complex and the Vam7 PX domain via two distinct sites. *Molecular biology of the cell*. 22:2601-2611.

Lachmann, J., F.A. Barr, and C. Ungermann. 2012. The Msb3/Gyp3 GAP controls the activity of the Rab GTPases Vps21 and Ypt7 at endosomes and vacuoles. *Molecular biology of the cell*. 23:2516-2526.

Lauwers, E., Z. Erpapazoglou, R. Haguenauer-Tsapis, and B. Andre. 2010. The ubiquitin code of yeast permease trafficking. *Trends in cell biology*. 20:196-204.

Li, S.C., and P.M. Kane. 2009. The yeast lysosome-like vacuole: endpoint and crossroads. *Biochimica et biophysica acta*. 1793:650-663.

Lo, S.Y., C.L. Brett, R.L. Plemel, M. Vignali, S. Fields, T. Gonen, and A.J. Merz. 2012. Intrinsic tethering activity of endosomal Rab proteins. *Nature structural & molecular biology*. 19:40-47.

Longtine, M.S., A. McKenzie, 3rd, D.J. Demarini, N.G. Shah, A. Wach, A. Brachat, P. Philippsen, and J.R. Pringle. 1998. Additional modules for versatile and economical PCR-based gene deletion and modification in Saccharomyces cerevisiae. *Yeast*. 14:953-961.

Luhtala, N., and G. Odorizzi. 2004. Bro1 coordinates deubiquitination in the multivesicular body pathway by recruiting Doa4 to endosomes. *The Journal of cell biology*. 166:717-729.

MacDonald, C., N.J. Buchkovich, D.K. Stringer, S.D. Emr, and R.C. Piper. 2012a. Cargo ubiquitination is essential for multivesicular body intralumenal vesicle formation. *EMBO reports*. 13:331-338.

MacDonald, C., D.K. Stringer, and R.C. Piper. 2012b. Sna3 is an Rsp5 adaptor protein that relies on ubiquitination for its MVB sorting. *Traffic*. 13:586-598.

Mayer, A., D. Scheglmann, S. Dove, A. Glatz, W. Wickner, and A. Haas. 2000. Phosphatidylinositol 4,5-bisphosphate regulates two steps of homotypic vacuole fusion. *Molecular biology of the cell*. 11:807-817.

Mayer, A., W. Wickner, and A. Haas. 1996. Sec18p (NSF)-driven release of Sec17p (alpha-SNAP) can precede docking and fusion of yeast vacuoles. *Cell*. 85:83-94.

Merz, A.J., and W.T. Wickner. 2004. Resolution of organelle docking and fusion kinetics in a cell-free assay. *Proceedings of the National Academy of Sciences of the United States of America*. 101:11548-11553.

Nickerson, D.P., C.L. Brett, and A.J. Merz. 2009. Vps-C complexes: gatekeepers of endolysosomal traffic. *Current opinion in cell biology*. 21:543-551.

Nordmann, M., M. Cabrera, A. Perz, C. Bröcker, C. Ostrowicz, S. Engelbrecht-Vandre, and C. Ungermann. 2010. The Mon1-Ccz1 complex is the GEF of the late endosomal Rab7 homolog Ypt7. *Current biology : CB*. 20:1654-1659.

Paumi, C.M., M. Chuk, J. Snider, I. Stagljar, and S. Michaelis. 2009. ABC transporters in Saccharomyces cerevisiae and their interactors: new technology advances the biology of the ABCC (MRP) subfamily. *Microbiology and molecular biology reviews : MMBR*. 73:577-593.

Piper, R.C., A.A. Cooper, H. Yang, and T.H. Stevens. 1995. VPS27 controls vacuolar and endocytic traffic through a prevacuolar compartment in Saccharomyces cerevisiae. *The Journal of cell biology*. 131:603-617.

Plemel, R.L., B.T. Lobingier, C.L. Brett, C.G. Angers, D.P. Nickerson, A. Paulsel, D. Sprague, and A.J. Merz. 2011. Subunit organization and Rab interactions of Vps-C protein complexes that control endolysosomal membrane traffic. *Molecular biology of the cell*. 22:1353-1363.

Porcelli, L., C. Lemos, G.J. Peters, A. Paradiso, and A. Azzariti. 2009. Intracellular trafficking of MDR transporters and relevance of SNPs. *Current topics in medicinal chemistry*. 9:197-208.

Prosser, D.C., K. Whitworth, and B. Wendland. 2010. Quantitative analysis of endocytosis with cytoplasmic pHluorin chimeras. *Traffic*. 11:1141-1150.

Raymond, C.K., I. Howald-Stevenson, C.A. Vater, and T.H. Stevens. 1992. Morphological classification of the yeast vacuolar protein sorting mutants: evidence for a prevacuolar compartment in class E vps mutants. *Molecular biology of the cell*. 3:1389-1402.

Robinson, J.S., D.J. Klionsky, L.M. Banta, and S.D. Emr. 1988. Protein sorting in Saccharomyces cerevisiae: isolation of mutants defective in the delivery and processing of multiple vacuolar hydrolases. *Molecular and cellular biology*. 8:4936-4948.

Sarry, J.E., S. Chen, R.P. Collum, S. Liang, M. Peng, A. Lang, B. Naumann, F. Dzierszinski, C.X. Yuan, M. Hippler, and P.A. Rea. 2007. Analysis of the vacuolar luminal proteome of Saccharomyces cerevisiae. *The FEBS journal*. 274:4287-4305.

Schiestl, R.H., and R.D. Gietz. 1989. High efficiency transformation of intact yeast cells using single stranded nucleic acids as a carrier. *Current genetics*. 16:339-346.

Schonthaler, H.B., V.C. Fleisch, O. Biehlmaier, Y. Makhankov, O. Rinner, R. Bahadori, R. Geisler, H. Schwarz, S.C. Neuhauss, and R. Dahm. 2008. The zebrafish mutant lbk/vam6 resembles human multisystemic disorders caused by aberrant trafficking of endosomal vesicles. *Development*. 135:387-399.

Seals, D.F., G. Eitzen, N. Margolis, W.T. Wickner, and A. Price. 2000. A Ypt/Rab effector complex containing the Sec1 homolog Vps33p is required for homotypic vacuole fusion. *Proceedings of the National Academy of Sciences of the United States of America*. 97:9402-9407.

Shields, S.B., and R.C. Piper. 2011. How ubiquitin functions with ESCRTs. *Traffic*. 12:1306-1317.

Starai, V.J., C.M. Hickey, and W. Wickner. 2008. HOPS proofreads the trans-SNARE complex for yeast vacuole fusion. *Molecular biology of the cell*. 19:2500-2508.

Stark, C., B.J. Breitkreutz, T. Reguly, L. Boucher, A. Breitkreutz, and M. Tyers. 2006. BioGRID: a general repository for interaction datasets. *Nucleic Acids Research*. 34:D535-539.

Stepp, J.D., K. Huang, and S.K. Lemmon. 1997. The yeast adaptor protein complex, AP-3, is essential for the efficient delivery of alkaline phosphatase by the alternate pathway to the vacuole. *The Journal of cell biology*. 139:1761-1774.

Stringer, D.K., and R.C. Piper. 2011. A single ubiquitin is sufficient for cargo protein entry into MVBs in the absence of ESCRT ubiquitination. *The Journal of cell biology*. 192:229-242.

Strochlic, T.I., B.C. Schmiedekamp, J. Lee, D.J. Katzmann, and C.G. Burd. 2008. Opposing activities of the Snx3-retromer complex and ESCRT proteins mediate regulated cargo sorting at a common endosome. *Molecular biology of the cell*. 19:4694-4706.

Theos, A.C., S.T. Truschel, D. Tenza, I. Hurbain, D.C. Harper, J.F. Berson, P.C. Thomas, G. Raposo, and M.S. Marks. 2006. A lumenal domain-dependent pathway for sorting to intralumenal vesicles of multivesicular endosomes involved in organelle morphogenesis. *Developmental cell*. 10:343-354.

Ungermann, C., B.J. Nichols, H.R. Pelham, and W. Wickner. 1998a. A vacuolar v-t-SNARE complex, the predominant form in vivo and on isolated vacuoles, is disassembled and activated for docking and fusion. *The Journal of cell biology*. 140:61-69.

Ungermann, C., K. Sato, and W. Wickner. 1998b. Defining the functions of trans-SNARE pairs. *Nature*. 396:543-548.

Urbanowski, J.L., and R.C. Piper. 1999. The iron transporter Fth1p forms a complex with the Fet5 iron oxidase and resides on the vacuolar membrane. *The Journal of biological chemistry*. 274:38061-38070.

Urbanowski, J.L., and R.C. Piper. 2001. Ubiquitin sorts proteins into the intralumenal degradative compartment of the late-endosome/vacuole. *Traffic*. 2:622-630.

Vida, T.A., and S.D. Emr. 1995. A new vital stain for visualizing vacuolar membrane dynamics and endocytosis in yeast. *The Journal of cell biology*. 128:779-792.

Wang, C.W., P.E. Stromhaug, E.J. Kauffman, L.S. Weisman, and D.J. Klionsky. 2003a. Yeast homotypic vacuole fusion requires the Ccz1-Mon1 complex during the tethering/docking stage. *The Journal of cell biology*. 163:973-985.

Wang, L., A.J. Merz, K.M. Collins, and W. Wickner. 2003b. Hierarchy of protein assembly at the vertex ring domain for yeast vacuole docking and fusion. *The Journal of cell biology*. 160:365-374.

Wang, L., E.S. Seeley, W. Wickner, and A.J. Merz. 2002. Vacuole fusion at a ring of vertex docking sites leaves membrane fragments within the organelle. *Cell*. 108:357-369.

Wemmie, J.A., and W.S. Moye-Rowley. 1997. Mutational analysis of the Saccharomyces cerevisiae ATP-binding cassette transporter protein Ycf1p. *Molecular microbiology*. 25:683-694.

Wickner, W. 2010. Membrane fusion: five lipids, four SNAREs, three chaperones, two nucleotides, and a Rab, all dancing in a ring on yeast vacuoles. *Annual review of cell and developmental biology*. 26:115-136.

Wurmser, A.E., T.K. Sato, and S.D. Emr. 2000. New component of the vacuolar class C-Vps complex couples nucleotide exchange on the Ypt7 GTPase to SNARE-dependent docking and fusion. *The Journal of cell biology*. 151:551-562.

Xu, H., and W.T. Wickner. 2012. N-terminal domain of vacuolar SNARE Vam7p promotes trans-SNARE complex assembly. *Proceedings of the National Academy of Sciences of the United States of America*. 109:17936-17941.

Zlatic, S.A., K. Tornieri, W. L'Hernault S, and V. Faundez. 2011. Metazoan cell biology of the HOPS tethering complex. *Cellular logistics*. 1:111-117.